International Journal of Recent Technology and Engineering (IJRTE)
ISSN: 2277-3878 (Online), Volume-8 Issue-4, November 2019

A Method for Autonomous Picking of Paper Reels

Meqdad H. M. Hasan

Abstract: ***Although aspects of this research had been presented and demonstrated the first time in 2011, the 'autonomous picking of objects' is still one of the hottest topics in this field. This research deals with the picking and handling of very large cylindrical objects such as paper reels or oil drums that are located inside industrial and commercial yards. It presents a new method for picking them autonomously according to their position, accessible direction, and surrounding barriers. Different terminology has been added to this research field. Three new algorithms; for picking a priority, for choosing the most appropriate direction for picking the target, and for choosing the safest path to reach the target without causing damage have been developed and implemented. The algorithms were tested successfully on simulation environment implemented using MATLAB and results taken from real experiments.***

Keywords : Autonomous picking, material handling, robotics, selection priority, unmanned vehicles

I. INTRODUCTION

Object grasping and picking has been extensively studied in the last two decades [1]. Robotic grasping is one of the most fundamental tasks of a robot and numerous studies have been carried on to enhance the robots ability to grasp a target object properly [2]. To achieve this task, "the robot needs to both perceive its surroundings correctly and decide on how to grasp the object based on its understanding. The robot usually resorts to using different sensors to perceive its environment" [3].

In industry, logistics automation is one of the active researches and development fields. In reality, the concept of automating logistic must means that all aspect of the completely automated material handling solution, including the loading/unloading phase are addressed. Thus, "industrial autonomous vehicles must be able to understand their surroundings and to cope with uncertainty" [4].

Research in the field of material transportation logistics and the need for picking algorithms is only one topic in the grasping and picking paradigm. Most research papers which discussed industrial autonomous forklifts were focused on traditional pallet picking [4],[5]–[7]. However, the need for handling materials of different kind and shape such as paper reels in paper mills encouraged researchers [8] to create a modified autonomous forklift by changing the forks into cylindrical clamps. This had made dealing with material picking and grasping somewhat different from the research and developments (R&D) that focus on the traditional forklifts.

This research was first presented in 2011 as part of the master's degree project. The work itself is to complement the MALTA project [8] and to find both the best direction and best priority for picking paper reals.

The following sections will review the previous work done on autonomous forklifts and pallet/object detection and, explain the reasons behind this work. Methods and explanations for object recognition, priority finding and picking direction algorithms will be discussed, results presented along with the conclusion.

A. Previous Works

Autonomous forklifts have great potential to offer improvements in terms of cost, safety, efficiency. The task of detecting pallets by sensors that are attached to the autonomous forklift is widely researched. It is one of the tasks that represents the greatest challenge. This is because completely or partially, previously as yet unknown environment, introduces a high degree of uncertainty to this task, making it less well defined. Therefore, more reliable, cost-effective and suitable sensors must be employed together with robust real-time algorithms. On the other hand, "faulty situations may also occur in highly repetitive and pre-determined tasks when, for example, a pallet lies in an unexpected position and a blind pick-up would cause a system fault and possible damage" [4].

Garibott et.al. [6] were the earliest who addresses the problem of pallet localization and picking through his work. The problem itself was not addressed individually but as a part of the complete system. Almost all later works [9], [10], [4], [5], [7], [11]–[22] and [23] followed the same procedure by considering the detection and picking problem as a sub-problem of the complete system. Varga et.al. [24]: "the technical literature for the specific task of pallet detection is scarce, almost non-existent". They were also the first who dealt with this specific aim as an individual task.

Manuscript published on November 30, 2019.
* Correspondence Author
Meqdad Hamdan Mohammad Hasan, Department of Building Engineering, College of Architectural and Planning, Imam Abdulrahman Bin Faisal University (IAU), Dammam, Saudi Arabia. Email: hmeqdad@iau.edu.sa

All previous researchers used various sensors for vision as the video camera, laser range finder (LRF), 3D time of flight cameras (ToF) and others or a combination of them (2 or 3 sensors together), which becomes current practice. They also proposed a wide variety of algorithms each based on the available sensors on their respective machines. Each of those systems has its advantages and weaknesses. For example, it was noted [24] that algorithm inputs should contain ”a pair of images, an operation point position request, information about operation type (the number of pallets, the level, number of reference points, storage type, pallet dimensions, 3D static map” which required a lot of previous information to be ready before letting the autonomous truck operate. Later, Andreasson et.el [15] and Stoyanova et. al. [23] noted that the autonomous grasping/ manipulation of unstructured goods at satisfactory cycle times are the key obstacles to overcome. Others, later, developed a system for loading/unloading pallets and objects or parcels from pallets to shelves [7]. The system truck included forks for pallet handling and a hand for parcels handling.

All those systems in the literature, dealt with a forklift with forks and either wooden or plastic pallets. Once the pallet tines are determined the picking problem becomes straight forward. The direction of the forklift at the moment of picking as well as the direction of picking is parallel and centered to the pallet face. To select the target pallet to be picked many algorithms had suggested, relying on labelling pallets with some kind of signs and labels, and internal systems for choosing and arranging the targets to be picked. However, the technical literature describing algorithms for both priority and direction of picking is so scarce, it may even be non-existent.

Abdelbaki et.al. [8] retrofitted an automated truck to handle heavy cylindrical materials such as paper reels, oil drums and huge wire rolls. Creating this truck raises the importance of further research to address the question regarding the picking direction. Cylindrical objects have a total of 360◦ of direction to be picked. The behaviour of loading/unloading for those objects also raises the problem of priority selection.

The detection and picking of autonomous picking of cylindrical objects had been described in the literature dealing with the aspect of grasping and manipulation by robotic arms and humanoid robots [25], [26]–[28] and [29] and many others, too numerous to list here, using different kind of cameras associated with algorithms depends on image processing and machine learning. Recent research [3] used image processing with deep learning. However, until the present, the author of this article is not aware of any published research to detect an object with the aim of grasping it associated with a humanoid robot or robotic arm using LRF.

The problem of grasp-planning is complex and extensively researched. Sahbani et. al. [1] and Bohg et. al. [2] classified grasp synthesis that can solve the grasp planning problem into two main categories. The model-analytical and the empirical approaches (Bohg named it data-driven approach) are complex, and both parametrize the grasp by, the grasping point on the object (named here as picking angle), the approach vector, the 3D angle as the robot hand approaches the grasping point with (referred to here as picking direction), with the wrist orientation of the robot hand (referred to as truck moving direction). The initial finger configuration step was not addressed in this research because the truck under investigation has only two grippers deals with only specific objects type and texture and the optimal grasping force was determined although not reported [8].

These two approaches were deemed to be too complex to be included in this research since the task of handling could be solved in 2D rather than at 3D level. The third dimension of this task can be neglected or/ incorporated easily by adding the height of objects that are needed to be handled. The objects usually has a constant height but the diameter of the cylinder is different. Hence, this paper addressed the problem at the 2D level only. Krug et.al [7] studied the grasp planning problem in 3D cylindrical object for the robotic arm attached to APPLE truck by confining the motion of the grippers to the 2D only , looked at grasping ability (this work refers to it as picking availability) as predefined pose envelope and by adding some constraints. However, the work never solved the question of grasping priority.

The work presented here contributes to the field of research by answering three major questions relating to the MALTA truck; which is the first paper reel has to be picked? From which direction should the truck approach a targeted paper reel? How to track the change in paper real stack counts that may be caused by other human-driven trucks in the warehouse?

B. Motivation and Related Works

The truck created by [8], [30] has grippers instead of forks to handle heavy cylindrical objects safely especially paper reels inside a warehouse. In their published paper they discussed the entire system but they did not focus on the picking problem itself. For loading-unloading of paper reels, they used a scenario to place reels inside a predefined loading zone by manually-driven truck and the MALTA truck could then pick and take them to a container. To achieve the assigned task, the truck started driving towards a predefined point where the online-computed path could be initiated. Once at point *A*, the closest reel was selected as a target to be approached and be picked up. To do that, the online navigation module requested the position of the selected reel, generated B-spline and then sent them to a controller [8] which ordered the truck to follow the generated trajectory. When the truck reached the target reel, the controller proceeded with the loading-unloading operation. To avoid the situation of the clamps hitting the reel when turning, the truck was forced to drive straight at the final part of the B-spline. The various issues faced in their work have been reported as follows:

- The paper reel anywhere in the warehouse should be autonomously loaded-unloaded, not only the once in the loading zone. The major problem facing them was that the locations of the reels are in constant change, which would make data association difficult.
- The use of predefined path was problematic and time-consuming. That is because the truck was not allowed to change path at run-time.

The above description demonstrates-that half the work is done manually, and the truck approaches the targeted reel all the time from the same direction. This may be the main reason why they needed to gather reels by manually-driven truck to a loading zone. The investigators also reported that warehouse pillars of the same size of paper reels are located among the stake of paper reels. Detecting these pillars in a 2D scanning causes, the truck controller to identify it as a paper reel which may require picking.

The main motivation for this work was to solve the issues that are described in the previous two paragraphs for MALTA trucks which were there at the time of doing this research in 2011. Hence, this research used the available sensors and algorithms on the MALTA truck and the work was confined to only limited changes to the algorithm to enable limited retrofitting for the truck. The author is not aware of any subsequent developments on MALTA trucks after and at the time of the preparation of this paper for publication.

II. METHODOLGY

To solve the problems presented, a simulation environment had been created on MatLab. It contained a hypothesized warehouse, a door and container, pillars of the warehouse and a hypothesized stack of paper reels. A truck with an LRF fitted on the middle of its front edge was then inserted into the environment.

With an assumption that 'there is no slip in motion' the robot was modelled like a bicycle with two wheels, a steering wheel in the back and a tracking wheel in the front. The robot position can be described by the coordinates of its location and its heading angle; vector $\boldsymbol{P}$. The positions of the paper reels and warehouse pillars are described by the same way as $\boldsymbol{P}_{reel}$.

A. Scans, Errors and Feature extraction

This section is based on works by [31], [32]. The simulated LRF sends and receives 360 beams with a precession of 0.5◦ and covers 180◦ with beam maximum range of 35m. Two normal distributed errors have been added; error to the robot position δP_{noisy} and error to the LRF readings $\boldsymbol{d}_{noisy}(i)$; where $\boldsymbol{d}(i)$ is the i^{th} beam reflection.

Two laser scanners were added to the simulation environment with the same error. The first one is fixed in the middle of the robots' forklifts and directed straight forward. This laser scanner covers directions of 180°'s. The other is fixed beside the first one but with a different orientation, covering an area of 270°'s, 135°'s from each direction. This is to aid detecting of the objects.

The segmentation process is done on the polar coordination system. The *Point Distance-Based Segmentation* method (PDBS) is used as described in [33].

After segmentation, each segment is fitted to one of two objects; line or circle. The process was done as in Fig. 1. Circle fitting was achieved by combining two different methods that were taken from the work of Chernov and Lesort [34] and [35] for fast and optimized circle detection. Accepting or rejecting of any fitted circle were made by testing each circle covariance matrix by the predefined threshold. The variance of the three variables of the circle should be less than three times the variance of the LRF as follows.

$$\left(\sigma_a^2 + \sigma_b^2 + \sigma_r^2\right) < \left(3 \times \sigma_R^2\right)$$

where σ_a^2 and σ_b^2 are the variance of x and y position of the centre of the circle respectively, σ_r^2 is the variance of the circle radius and σ_R^2 is the variance of LRF distance range.

The line fitting is done according to the weighted linear regression method as mentioned in [36]. The acceptable line is the extracted line which has a covariance matrix that has the following condition.

$$\left(\sigma_\alpha^2 + \sigma_d^2\right) < \left(2 \times \sigma_R^2\right)$$

where α is the direction of the line, d is the perpendicular distance from the robot to the line and σ_R^2 is the variance of the LRF range.

Finally, all extracted circles are compared to predefined range of diameters. These predefined range of diameters were designed to describe and cover all possible range of paper reels diameters and the tolerance at each diameter. Once the extracted circle's diameter falls outside this predefined range the extracted circle is ignored.

B. Map Updating

Once all features from the laser scanners were extracted the process of map building starts. The map building algorithm steps were as follows:

1) Build a local map from the extracted features at each LRF's scan.
2) At a robot coordinate system, apply matching algorithms to match both current extracted maps from the two LRFs' scans and add all objects from both scans to the local map.
3) At a robot coordinate system, apply a matching algorithm to match the current extracted map to previous extracted map from the previous scan.
4) Update the local map with newly appeared/ disappeared objects.
5) Convert the resulting map to the global coordinate system.
6) At the global coordinate system compares the current map with the previous global map if there.

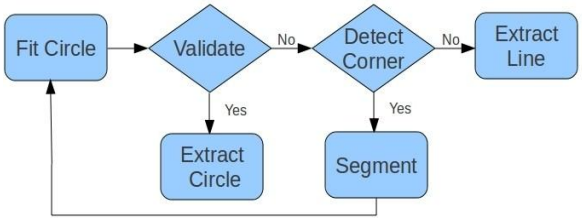

Fig. 1. Feature extraction algorithm flow chart.

7) Update the global
8)
9)
10) map with newly appeared/ disappeared objects.
11) Compare the final global map to a predefined map of the warehouse.
12) At the global map match lines to walls of the warehouse (label them as walls), describe other lines as obstacles. Then find the circles that match the warehouse pillars, label them as pillars and describe other circles as paper reels.

At the end of the process, the robot will have an updated global map with labels for all appeared objects and location of them. **Error! Reference source not found.** describes the matching algorithm that is used to match and update local maps using Kalman filter [37] in its static mode. The updating algorithm steps were:

1) Transfer features that were considered as paper reels from previous sample time and from new sample time to the LRF1 frame.
2) For each paper reel inside the LRF's range, find its corresponding one from the new map.
3) If there is a paper reel in the same location in the previous map but not in the new one, remove the reel from the global map.
4) If there is a paper reel in the new map but not in the previous map update the global map by adding the new one.

To keep tracking of all newly added and newly removed paper reels in the environment; the paper reels are extracted to a special data structure. In each localization step, and by using the dynamic mode of the Kalman filter, the new location of the robot itself and the new location of each paper reel in the data structure is predicted according to the velocity and direction of the robot. If the predicted step does not predict a paper reel but one is detected by the scanners, a new paper reel is added to the data structure and hence to the map. If a paper real is found in the data structure, and its new location is predicted, but there is no update stage for it, i.e. it does not appear in the scanner's images, this paper reel is directly removed from the data structure and hence from the map. To avoid the situation of removing paper reels which are not in the LRF ranges, the main effort was concentrated on keeping track of only those reels that locate within the range of LRF's scanners [37].

C. Path Selection

To avoid damage of paper reels resulting from a crash between the truck and paper reels and because of the curving nature of the B-spline function, 6 points instead of 4 [38], [39] have been chosen as shown in **Fig. 2**. $\boldsymbol{P_1}$ is the centre of rotation of the robot. $\boldsymbol{P}_2$ is the centre point of the robot's two forks. To ensure straight forward motion and to avoid rotation in very close angle (which although is impossible in real environment), $\boldsymbol{P}_3$ is chosen to be in front of the truck in the same heading direction, at a distance to the truck equal to *1.5* times the length of truck (*1.5d*). This distance was measured from the truck's centre of the rotation. $\boldsymbol{P}_6$ is chosen to be the centre of the target paper reel to be picked. $\boldsymbol{P}_5$ is

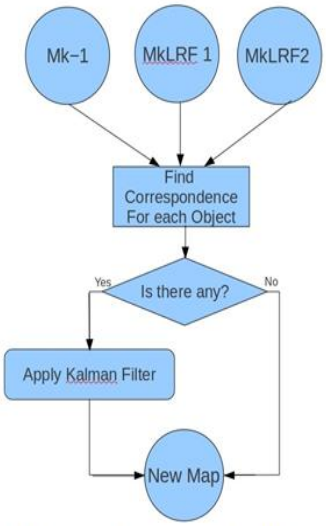

Fig. 2. Matching algorithm flow chart. M_{k-1} is the previous local map. M_{kLRF1}: is the current extracted map from first LRF. M_{kLRF2}: is the current extracted map from second LRF

chosen to be on the circumference of the reel in the same direction, from where the reel is to be picked up (***Picking Direction***). $\boldsymbol{P}_4$ is chosen to be at the same picking direction of the paper reel and at *1.5* times the length of the truck from the circumference of the paper reel. This point is chosen to ensure that the paper reel is reached in a safe, smooth and straight-forward manner, avoiding sudden rotation at such close proximity to the reels.

The reverse-path is the path to the loading area. This path is generated the same way as above but with extra points, as in Fig. 3. Three extra points are added to the B-spline function used above. These three points are used to define the loading area location. $\boldsymbol{P}_5$ is a random point in the centre of the loading area door. A point in the place of the loading area is given in the predefined map. The accurate zone of the loading area is generated in the global map that is generated in II.B. The fourth point $\boldsymbol{P}_4$ is chosen at *1.5* times the truck length from $\boldsymbol{P}_5$ in the same direction as the direction the loading zone but to the outside of it. $\boldsymbol{P}_6$ is the mirror point to $\boldsymbol{P}_4$ and inside the loading area.

The map building algorithm returns the coordinates and borders of the loading area and its occupied locations as part of the global map. The loading area is divided into virtual cells. Each cell is a square with side dimensions equalling the diameter of the paper reel plus a safe distance for truck grippers. The loading algorithm is made to fill the farthest row starting from the first empty location. The loading path to the first empty location of the farthest row of the loading area grid as described by the following nine points:

$$Path_{Loading} = \begin{bmatrix} P_1 = (C_x, C_y)_t \\ P_2 = (C_x, C_y)_t - r_t e^{i\alpha_t} \\ P_3 = (C_x, C_y)_t - (r_t + 1.5d) e^{i\alpha_t} \\ P_4 = P_5 - 1.5de^{i\gamma} \\ P_5 \\ P_6 = P_5 + 1.5de^{i\gamma} \\ P_7 = E_{cell} - (r_t + 1.5d) e^{i\gamma_t} \\ P_8 = E_{cell} - r_t e^{i\gamma_t} \\ P_9 = E_{cell} + r_t e^{i\gamma_t} \end{bmatrix} \quad (1)$$

Where

$$I_{lc} + \frac{w}{2} e^{i(\gamma - \frac{\pi}{2})} \le P_5 \le I_{lc} - \frac{w}{2} e^{i(\gamma - \frac{\pi}{2})} \quad (2)$$

Where $(C_x, C_y)_t$ is the centre of paper reel number *t*, *t = 1, 2, 3...n* and *n* is the total number of paper reels in the stack. $\boldsymbol{P}_5$ is a random point on the loading area entrance. It should satisfy the condition as described in (2). $\boldsymbol{I}_{lc}$ is the left hand side entrance coordinate. $\boldsymbol{I}_{rc}$ is the coordinate to the right hand side entrance. $\boldsymbol{\gamma}$ is the container orientation. *w* is the truck total width. '*d*' is the truck total length. Ecell is the nearest edge of the farthest unoccupied cell in the loading area. 'r_t' is the paper reel radius. α_t is the picking direction of the target reels as in section II.D. The return path is described in the same way but in reverse order.

$$Path_{return\_back} = [P_9, P_8, P_7, P_6, P_5, P_4, P_3, P_2, P_1]^T$$

Points $\boldsymbol{P}_1$, $\boldsymbol{P}_2$ and $\boldsymbol{P}_3$ are calculated according to the location and picking direction of the new targeted paper reel *t +1*.

D. Method for Selecting Paper Reels Priority

Some new terminologies have been developed and imported to the algorithm to guarantee a smooth, accurate operation.

i. *Terms and Definition*

Obstacle is any objects (described as a line or a circle in the global map) that is located in a distance of the target reel less than or equal to *1.5* times the length of the truck.

Picking direction (θ) is the heading angle θ of the truck at the moment of picking the target.

Availability denotes all possible angles of picking directions, where the truck can navigate to easily and safely, without obstacle in the way of that picking direction.

Picking interval ***(a)*** is the total sum of angles in degrees that the designer can consider as one direction at the moment of picking. The smaller this interval, the better result.

Accessibility angle ***(γ)*** is the central angle of the paper reel which is opposite to the direction of picking provided, that the coordinate system origin is the centre of the paper reel. Thus $\theta = \gamma + \pi$.

Centre to centre distance is the shortest distance between the centre of the target reel to the centre of obstacle in case of a circular obstacle. If the obstacle is linear, the centre to centre distance is the shortest distance to the surface of that obstacle.

Centre to centre angle is the angle between the centre line and the x axis of the global map in the case of a circular obstacle.

'ε' is the angle between the picking direction and the centre line.

ii. *Reel Priority and Reel Directions*

Once the previous step had finished, all reels in the unloading area are inspected to select **the nearest most accessible reel**. To accomplish that, a five-stage algorithm is created as follows:

1) Find all accessible reels in the internal data structure.
2) Find the nearest one of the accessible reels.
3) Generate paths to all possible accessibility angles of the nearest accessible reel by using path generating algorithm.
4) The shortest path is the path of the truck.
5) As each new reel appears, update the path of the truck by repeating steps (1,2,3,4) to two reels only (the selected reel and the newly appearing reel).

"Before calculating the accessibility, each target reel is assumed to be accessible from 360°. For the sake of saving both computational power and memory space, the assumption was to check accessibility at intervals, which was sufficient enough to give clear evidence about what direction was accessible. Each paper reel has been given 72 accessible direction by steps of 5°. This starts from 0° direction (positive x access on the global map) to 359°, see **Fig. 4**. Accessibility direction of paper reels means that the truck has to be able to manoeuvre if it moves toward the reel from that direction. The truck is able to manoeuvre freely if the shortest distance between the surface of the reel and any obstacle surface is more than *1.5* times of the total truck length" [37] .

Obstacles could be walls, columns or other paper reels. If the distance between any obstacle and the reel is less than *1.5* times the total length of the truck, then the accessibility angle can be calculated according to the following procedure. In the case of paper reel or column obstacle, the algorithm calculates the maximum and minimum picking direction according to the belt problem [40], see Fig. 7 The two angles are described as follows:

$$\varepsilon = \sin^{-1}\left(\frac{r_1 + r_2 + g}{P}\right)$$
$$\theta_{\max} = roundUP\left(\frac{modulus((\pi + \phi + \varepsilon), 2\pi)}{a}\right) \times a$$
$$\theta_{\min} = roundDown\left(\frac{modulus((\pi + \phi - \varepsilon), 2\pi)}{a}\right) \times a \quad (3)$$
$$\phi = \tan^{-1}\left(\frac{y_2 - y_1}{x_2 - x_1}\right)$$

where *(a)* is the picking interval. If the obstacle is a large surface such as walls or any other bulky circular object which is greater than predefined radius in the above suggestions, the shortest distance between the centre of the "reel and the obstacle is the perpendicular distance to that obstacle. The direction of robot movement (picking direction), between the reel and the obstacle creates a triangle as appears in **Fig. *6***.

Fig. *6* shows that the inaccessible directions are located between obstacle, reel and two picking angles say Θ_{min} and Θ_{max}. If the minimum required distance, that allows manoeuvring is 1.5*d* -where *d* is the total length of the truck- is considered" [37], then the equations (3) become as in equations (4)

$$\varepsilon = \sin^{-1}\left(\frac{P+r+2g}{d+2g}\right)$$

$$\theta_{\max} = roundUP\left(\frac{\text{modulus}\left(\left(\lambda+\frac{\pi}{2}-\varepsilon\right),2\pi\right)}{a}\right)\times a \qquad (4)$$

$$\theta_{\min} = roundDown\left(\frac{\text{modulus}\left(\left(\lambda-\frac{\pi}{2}+\varepsilon\right),2\pi\right)}{a}\right)\times a$$

where λ is the obstacle norm global direction. g is the thickness of the truck groupers.

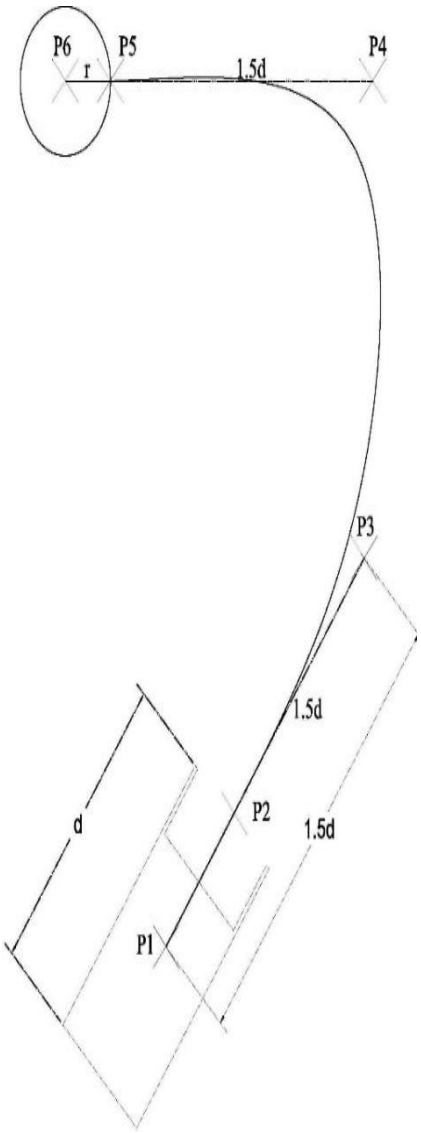

Fig. 2.The six points that are chosen to generate the robot's path to any paper reel and their arrangements.

Finally, to determine the accessibility angle, γ, the following definition had been made. The picking angels are a set of angles in "*a*" intervals from Θ_{min} to Θ_{max} moving clockwise and including both of Θ_{max} and Θ_{min}. The accessibility angle γ is the picking angle plus 180°. The example in the appendix demonstrates the concept above.

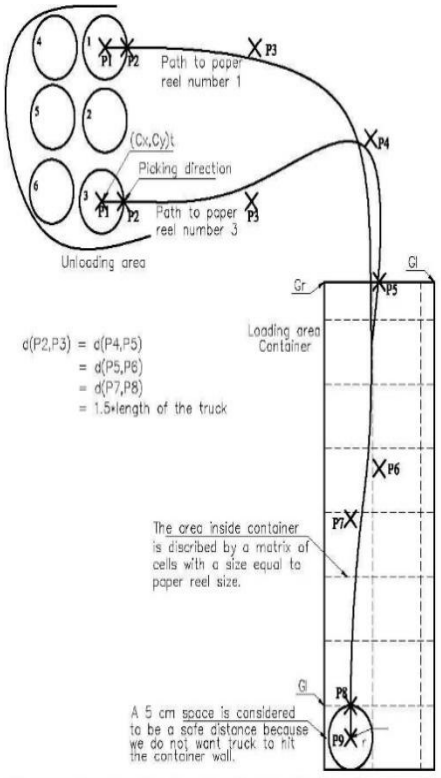

Fig. 3. The path selection to transport reels from the unloading, to the loading area. The path is described by 9 points P_1, P_2 and P_3 as points (P_4 ,P_5 and P_6) in Fig. 2. 3 points (P_4,P_5 and P_6) to guide the vehicle through the container entrance. Other 3 points (P_7, P_8 and P_9) to guide the vehicle to the farthest unoccupied cell in the container[37]

III. RESLTS

The working environment has been modelled as mentioned above and thus the truck was fitted with the two laser scanners. The scans of the two laser scanners were taken to the segmentation process. The P DBS segmentation process was chosen as mentioned previously [34] because it is the robust algorithm for this environment. After different tests, the value of the noise reduction constant Co in the algorithm was selected to be equal to the error of the LRF. The error in the segmentation algorithm has been optimized especially on the fringe and on the nearest segments. Table I shows the results.

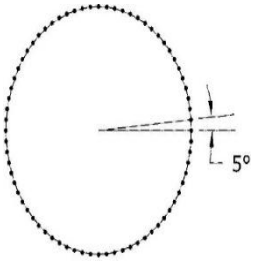

Fig. 4. Each reel has a 360◦ accessibility angles. Instead, it is considered as interval. Thus each reel has a small number of accessibility angles spread on the reel circumstance [37].

The features were fitted directly from extracted segments. Features with high uncertainty were rejected by the algorithm. However, this did not affect the final results because of cumulative behaviour of the map building algorithm. Table II shows the result of fitting a circle and line. Note that the resulted error had been decreased to the minimum. Fig. 5 shows the result of segmentation and feature extraction algorithms.

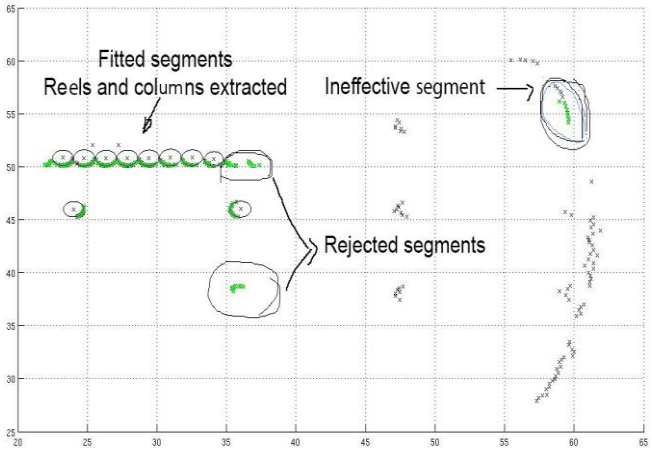

Fig. 5. Extracting features and building a local map. Notice the ineffective segments on the periphery and the rejected segments.

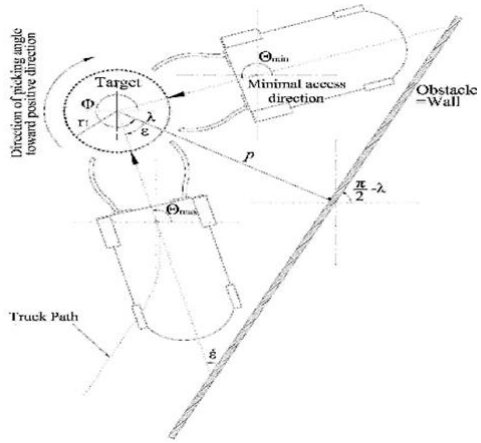

Fig. 6. Behaviour of truck-obstacle-reel at the moment of the grasping action if the obstacle is linear (wall)

Table I. A comparison between segmentation results;"number of effective segments and length of segments" when three values of noise reduction constants are used. The ineffective segments are segments on the beams fringes [37].

C_0	$0.5\sigma_r$	σ_r	$1.5\sigma_r$
Total number of segments	12	15	17
Number of effective segments	6	8	8
Number of ineffective segments	6	8	9
Number of incorrect segments	4	1	2
Average length of a segment	10.9	12.2	13.6
Average length of an effective segment	10.8	13	15.3
Number of unconsidered scan points(of 360)	229	177	129

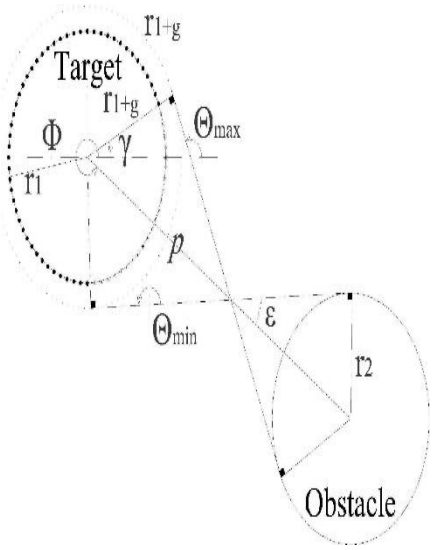

Fig. 7. Behavior of truck-obstacle-reel at the moment of grasping action if the obstacle is circular obstacle (warehouse pillar or another paper reel). The dots refer to the possible picking direction. The ×'s refer to inaccessible direction.

The use of Kalman filter to merge maps together as mentioned above, decreases the uncertainty in estimation to a minimum. It also makes rejection of segments more reliable and segments become more precise as they get closer to the truck. Thus, they appear in newer maps and therefore in the final map.

Fig. 9 shows the result of building a global map with no prior knowledge about the environment. The map in this figure is built from 112 scan image from two different LRFs while the robot moving from point (10,10) to point (30,50) in an almost straight line. **Table III** shows the enhancement in the uncertainty of objects after the map building process. Note that some features overlap each other. These

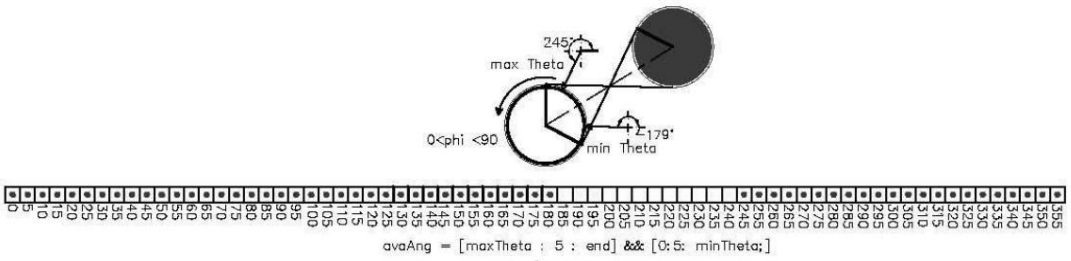

Fig. 8. Changing the presentation of accessibility angles to linear presentation then removing the inaccessible angles and flagging them.

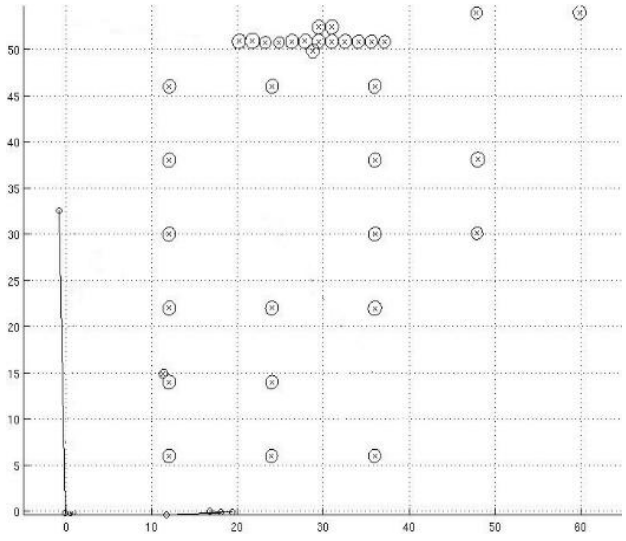

Fig. 9. The result of building a global map of 56 positions of the truck without any prior knowledge about the working environment.

overlapped objects are processed in the matching algorithm.

In the matching algorithm, it was found that some features that should have been extracted as line are extracted as circles and vice versa. Thus, a new step to the matching algorithm was added as follows; *[Calculate the perpendicular distance between each circle and each line in the map. If the distance is less than the radius of the circle, then calculate the intersection between the line and the circle. If there is an intersection or overlap then remove the object with the lower sum of uncertainty matrix diagonal line]*. The results had been noticeably improved. The updating process suggested above gave good results.

Table II. The uncertainty of features' parameters that followed from fitting segments into features.

Feature #	Uncertainty		
	U_{Cx}	U_{Cy}	U_R
$Column_1$	0.0029	0.0057	0.0046
$Column_2$	0.0010	0.0071	0.0054
Paper Real	$0.0474 *10^{-3}$	$0.1713 *10^{-3}$	$0.1485 *10^{-3}$
Wall	0.3644	0.0001	

However, there were some features which were extracted by mistake because of the error in the segmentation algorithm. These features are removed during the map-updating algorithm.

The three consequential maps needed a lot of computational power and memory space. Implementing of this algorithm was found to be very difficult on the simulated environment. The algorithm was tested separately outside of the simulation process. The first three maps were used to generate the first global map. Once the fourth local map is extracted the first local map was deleted and the second local map becomes the first one, and so on. The extracted features were compared to each new-extracted features. Generally, the algorithm could decrease the segmentation error in the total process.

The calculation of the priority of the paper reels and the picking direction was made from a fixed location for easy implementation. The results were as expected. **Fig. 12** and **Fig. 13** show the results of calculating the availability of each paper real in the stack after generating the global map, at prior to removing the first paper reel from the stack followed by removing the second one. Note how the Updating Algorithm finds the paper reel at the back of the first reel. The process of updating- calculating- choosing-moving continued until the desired stack had finished. The bold pink coloured dots in Fig. 12 and **Fig. 13** show the availability intervals. Note the paper reel at (36, 52) appears in **Fig. 13** but not in **Fig. 12** where it is extracted and added to the map there. Hence, it has not appeared in **Fig. 12** because it is surrounded by two other reels, thus it could not be seen. The paper reels in the top row except the two corners are not available because they are very near to a wall or because there is a warehouse pillar blocking the way of the truck. The availability of paper reels in location (36, 51) increased noticeably after moving paper reel number 13, **Fig. 13**. In general, the paper reel that has the least number of inaccessible directions is the most available paper reel. **Fig. 11** shows a closed look to the calculated picking interval for the paper reel in the left lowest corner of the stack.

Table III. The position and uncertainty of some features in map Fig. 9. These features are represented in a right place as appears.

Parameters			Uncertainty		
C_x	C_y	R	U_{C_x}	U_{Cy}	U_R
35.992	46.000	0.7446	$10^{-4}\times$ 0.15	$10^{-4}\times$0.039	$10^{-4}\times$0.11
35.597	50.814	0.7058	$10^{-03}\times$ 0.14	$10^{-03}\times$ 0.48	$10^{-03}\times$0.5
32.526	50.845	0.7443	$10^{-04}\times$ 0.051	$10^{-04}\times$0.091	$10^{-04}\times$0.117
23.217	50.717	0.6564	$10^{-03}\times$ 0.077	$10^{-03}\times$0.447	$10^{-03}\times$0.276

To calculate the nearest paper reel in the simulation environment, the straight distance from the truck initial position to the paper reels stack is considered. Thus the shortest straight distance from the truck's location first to the paper real, then to the centre of the loading zone becomes the deciding factor for selecting the first paper reel that should be moved. Of course, the result changes when the initial location of the truck changes. However, the above calculated assumption is still valid for the next paper reel when the truck drops its carriage in the loading area and returns to pick up the second paper reel where the calculation starts from the entrance of the loading area. **Fig. 13** shows that the paper reel in the lowest right corner was the first reel selected and moved as expected. In a subsequent step, the paper reel in location (36, 51) was the second one selected.

The path of the truck was generated as described above to fulfil the safety requirements. Fig. 14 shows a closer look at the results of the paths generated to each accessible direction.

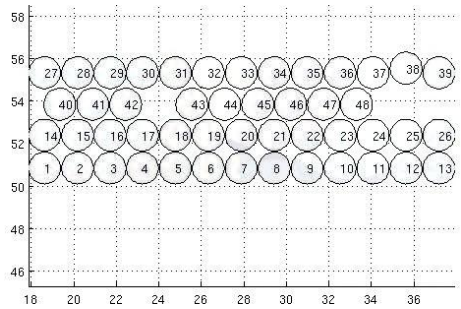

Fig. 10. The initial arrangements of paper reels without column..

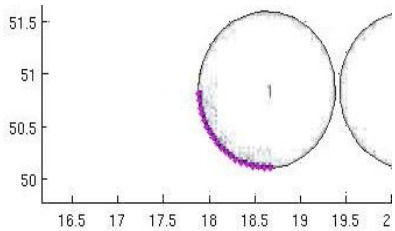

Fig. 11. A closer look at the picking angles and access.

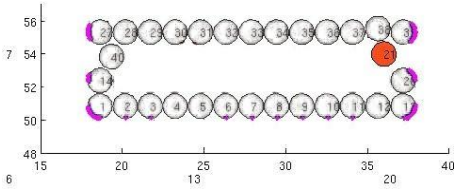

Fig. 12. First calculation of availability of paper

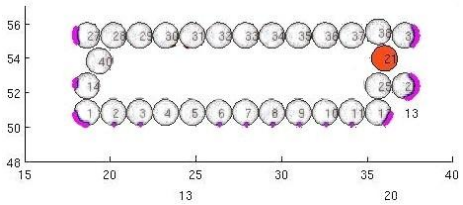

Fig. 13. Calculating of availability of paper reels after removing the first reel in stack..

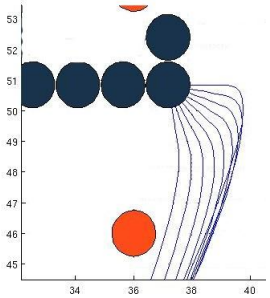

Fig. 14. All possible paths to the paper reel.

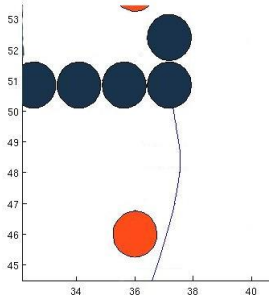

Fig. 15. The chosen path is the shortest and the easiest from paths in figure 15.

The total length of each path is calculated then the shortest path is chosen as in **Fig. 14** and **Fig. 15**. Unfortunately, during the research phase, it was not possible to update the truck's path automatically. Thus for convenience, the entrance of the loading area was chosen to be the starting point to calculate the first path for the first reel. However, for the next reel, the location of the truck after dropping down the previous reel inside the loading area was chosen to be the starting point for the next path for the next paper reel and so on. It appears from the figures above how the end of the path is almost a straight line to ensure safe manoeuvring to the paper reel.

IV. CONCLUSION

This work focused essentially on two problems; namely, how to choose the target paper reel to be picked and what are the best picking directions for the task? The results, as described above proved that the algorithm worked as well as expected. The results demonstrate the robustness of the algorithm for performing the tasks required.

The research also provided an example to demonstrate how this algorithm works. The algorithm is tested in both a simulation environment and by real data collected from a warehouse by MALTA. The results were encouraging. It showed that it was possible to extend the applications of this algorithm into a different kind of industry such as drums that are used for transporting oil or chemical materials, and for picking applications of cable reels, or cans. Nevertheless, further research may lead to progress and future advances in this field.

APPENDIX A. DEMONSTRATION EXAMPLE

Take Fig. 17 as an example to demonstrate the idea above. If the truck detected a paper reel of radius r = 0.897m, located at 2.085m from a wall and has 3.48m from the nearest paper reel. The later one has r = 0.95m. If the truck total length is 3.7m and the grabber width is 0.05m. The truck has updated its knowledge base with the following information: The location of the obstacle paper reel is at Φ = 210° from the targeted paper real, the location of the paper reel according to the wall is at λ =90° . The picking interval a = 5° is defined by the manufacturer.

Note: *It is not important to use degrees system or radian systems. The degree systems used here are only for demonstration purposes. The radian system is used for real application.*

Direct application to (4) leads to the following.

$$\varepsilon_1 = \sin^{-1}\left(\frac{p-r-2g}{d+2g}\right) = \sin^{-1}\left(\frac{208.5-89.7-10}{370+10}\right) = 16.64^\circ$$

$$\theta_{1-\max} = roundUP\left(\frac{\text{mod}(-90+90-16.64,360)}{5}\right)\times 5 = 345^\circ$$

$$\theta_{1-\min} = roundDown\left(\frac{\text{mod}(-90-90+16.64,360)}{5}\right)\times 5 = 195^\circ$$

Thus, the picking angle from the wall are all directions

[195 : 5 : 345]

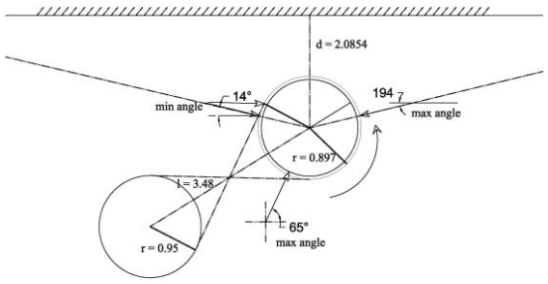

Fig. 17. A target paper reel with two obstacles; a wall and other paper reel.

Now to calculate the picking angle from the other paper reel,

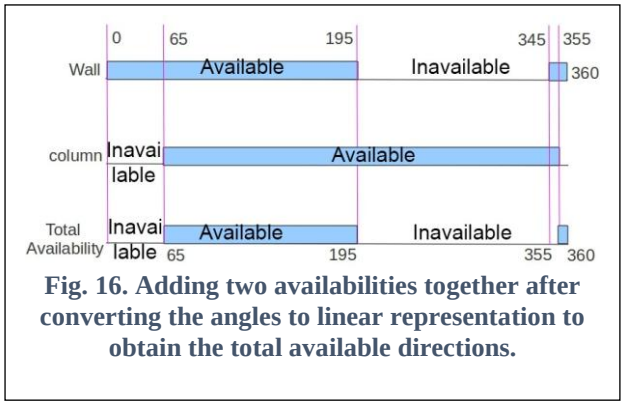

Fig. 16. Adding two availabilities together after converting the angles to linear representation to obtain the total available directions.

use (3) as follows.

$$\varepsilon_2 = \sin^{-1}\left(\frac{r_1+r_2+g}{P}\right) = \sin^{-1}\left(\frac{89.7+95+5}{348}\right) = 33.03^\circ$$

$$\theta_{2-\max} = roundDown\left(\frac{\text{mod}(90+210+33.03,360)}{5}\right)\times 5 = 65^\circ$$

$$\theta_{2-\min} = roundDown\left(\frac{\text{mod}(90+210-33.03,360)}{5}\right)\times 5 = 355^\circ$$

Thus the picking angle from the other paper reel becomes the interval of angles

[65 : 5 : 355]

Now by removing the unavailable angles from the two intervals above, where interval of angles (15 : 5 : 165) not available from the wall and interval of angles (5 : 5 : 65) not available from the other paper reel, the following intervals where the availability angles of the targeted paper reel.

[65 : 5 : 195] and [355 : 5 : 360]

Fig. 16 illustrates how both picking angles have been converted to linear representation then added together to find out the total picking intervals.

REFERENCES

1. A. Sahbani, S. El-Khoury, and P. Bidaud, "An overview of 3D object grasp synthesis algorithms," *Rob. Auton. Syst.*, vol. 60, no. 3, pp. 326–336, 2012.
2. J. Bohg, A. Morales, T. Asfour, and D. Kragic, "Data-Driven Grasp Synthesis—A Survey," *IEEE Trans. Robot.*, vol. 30, no. 2, pp. 289–309, Apr. 2014.
3. D. Guo, F. Sun, B. Fang, C. Yang, and N. Xi, "Robotic grasping using visual and tactile sensing," *Inf. Sci. (Ny).*, vol. 417, pp. 274–286, 2017.
4. L. Baglivo *et al.*, "Autonomous pallet localization and picking for industrial forklifts: a robust range and look method," *Meas. Sci. Technol.*, vol. 22, no. 8, p. 85502, 2011.
5. D. Lecking, O. Wulf, and B. Wagner, "Variable Pallet Pick-Up for Automatic Guided Vehicles in Industrial Environments," in *Emerging Technologies and Factory Automation, 2006. ETFA '06. IEEE Conference on*, 2006, pp. 1169–1174.
6. G. Garibott, S. Masciangelo, M. Ilic, and P. Bassino, "ROBOLIFT: a vision guided autonomous fork-lift for pallet handling," in *Intelligent Robots and Systems '96, IROS 96, Proceedings of the 1996 IEEE/RSJ International Conference on*, 1996, vol. 2, pp. 656–663 vol.2.
7. R. Krug *et al.*, "The Next Step in Robot Commissioning: Autonomous Picking and Palletizing," *IEEE Robot. Autom. Lett.*, vol. 1, no. 1, pp. 546–553, Jan. 2016.

8. B. Abdelbaki, A. Henrik, L. A. J., Å. Björn, and R. Thorsteinn, "MALTA: a system of multiple autonomous trucks for load transportation," in *Proceedings of the 4th European conference on mobile robots (ECMR)*, 2009, pp. 93–98.
9. R. Cucchiara, M. Piccardi, and A. Prati, "Focus based Feature Extraction for Pallets Recognition," 2000.
10. W. S. Kim, D. Helmick, and A. Kelly, "Model based object pose refinement for terrestrial and space autonomy," 2001.
11. M. R. Walter, S. Karaman, E. Frazzoli, and S. Teller, "Closed-loop pallet manipulation in unstructured environments," in *2010 IEEE/RSJ International Conference on Intelligent Robots and Systems*, 2010, pp. 5119–5126.
12. H. Son, C. Kim, and K. Choi, "Rapid 3D object detection and modeling using range data from 3D range imaging camera for heavy equipment operation," *Autom. Constr.*, vol. 19, no. 7, pp. 898–906, 2010.
13. C. Prasse, S. Skibinski, F. Weichert, J. Stenzel, H. Müller, and M. ten Hompel, "Concept of automated load detection for de-palletizing using depth images and RFID data," in *2011 IEEE International Conference on Control System, Computing and Engineering*, 2011, pp. 249–254.
14. F. Weichert *et al.*, "Automated detection of euro pallet loads by interpreting PMD camera depth images," *Logist. Res.*, vol. 6, pp. 99–118, 2013.
15. H. Andreasson *et al.*, "Autonomous Transport Vehicles: Where We Are and What Is Missing," *IEEE Robot. Autom. Mag.*, vol. 22, no. 1, pp. 64–75, Mar. 2015.
16. S. Byun and M. Kim, "Real-Time Positioning and Orienting of Pallets Based on Monocular Vision," in *2008 20th IEEE International Conference on Tools with Artificial Intelligence*, 2008, vol. 2, pp. 505–508.
17. J. Nygards, T. Hogstrom, and A. Wernersson, "Docking to pallets with feedback from a sheet-of-light range camera," in *Proceedings. 2000 IEEE/RSJ International Conference on Intelligent Robots and Systems (IROS 2000) (Cat. No.00CH37113)*, 2000, vol. 3, pp. 1853–1859 vol.3.
18. J. Pagès, X. Armangué, J. Salvi, J. Freixenet, and J. Martí, "9th Mediterranean Conf. on Control and Automation, MED'2001 (Dubrovnik, Croatia," in *2006 IEEE Conference on Emerging Technologies and Factory Automation*, 2001.
19. L. Baglivo, N. Bellomo, E. Marcuzzi, M. Pertile, and M. De Cecco, "Pallet Pose Estimation with LIDAR and Vision for Autonomous Forklifts," in *IFAC Proceedings Volumes (IFAC-PapersOnline)*, 2009, vol. 13.
20. M. Seelinger and J.-D. Yoder, "Automatic Visual Guidance of a Forklift Engaging a Pallet," *Robot. Auton. Syst.*, vol. 54, no. 12, pp. 1026–1038, Dec. 2006.
21. C. Pradalier, A. Tews, and J. Roberts, "Vision-based operations of a large industrial vehicle: Autonomous hot metal carrier," *J. F. Robot.*, vol. 25, no. 4-5, pp. 243–267, 2008.
22. L. Baglivo, N. Bellomo, G. Miori, E. Marcuzzi, M. Pertile, and M. De Cecco, "An object localization and reaching method for wheeled mobile robots using laser rangefinder," in *2008 4th International IEEE Conference Intelligent Systems*, 2008, vol. 1, pp. 5–11.
23. T. Stoyanov *et al.*, "No More Heavy Lifting: Robotic Solutions to the Container Unloading Problem," *IEEE Robot. Autom. Mag.*, vol. 23, no. 4, pp. 94–106, Dec. 2016.
24. R. Varga and S. Nedevschi, "Vision-based autonomous load handling for automated guided vehicles," in *2014 IEEE 10th International Conference on Intelligent Computer Communication and Processing (ICCP)*, 2014, pp. 239–244.
25. D. Berenson, R. Diankov, Koichi Nishiwaki, Satoshi Kagami, and J. Kuffner, "Grasp planning in complex scenes," in *2007 7th IEEE-RAS International Conference on Humanoid Robots*, 2007, pp. 42–48.
26. R. Krug *et al.*, "Velvet fingers: Grasp planning and execution for an underactuated gripper with active surfaces," in *2014 IEEE International Conference on Robotics and Automation (ICRA)*, 2014, pp. 3669–3675.
27. S. S. Srinivasa *et al.*, "HERB: a home exploring robotic butler," *Auton. Robots*, vol. 28, no. 1, p. 5, Nov. 2009.
28. D. Berenson, S. Srinivasa, and J. Kuffner, "Task Space Regions: A framework for pose-constrained manipulation planning," *Int. J. Rob. Res.*, vol. 30, no. 12, pp. 1435–1460, 2011.
29. R. Balasubramanian, L. Xu, P. D. Brook, J. R. Smith, and Y. Matsuoka, "Physical Human Interactive Guidance: Identifying Grasping Principles From Human-Planned Grasps," *IEEE Trans. Robot.*, vol. 28, no. 4, pp. 899–910, Aug. 2012.
30. A. Bouguerra, H. Andreasson, A. J. Lilienthal, B. Astrand, and T. Rognvaldsson, "An autonomous robotic system for load transportation," in *Emerging Technologies Factory Automation, 2009. ETFA 2009. IEEE Conference on*, 2009, pp. 1–4.
31. J. Ryde and H. Hu, "Laser based simultaneous mutual localisation for multiple mobile robots," in *Mechatronics and Automation, 2005 IEEE International Conference*, 2005, vol. 1, p. 404–409 Vol. 1.
32. L. Teslić, G. Klan\ucar, and I. \uSkrjanc, "Simulation of a Mobile Robot with an LRF in a 2D Environment and Map Building," in *Robot Motion and Control 2007*, vol. 360, K. Kozlowski, Ed. Springer Berlin / Heidelberg, 2007, pp. 239–246.
33. C. Premebida and U. Nunes, "Segmentation and Geometric Primitives Extraction from 2D Laser Range Data for Mobile Robot Applications," *Sci. Technol.*, pp. 17–25, 2005.
34. N. Chernov and C. Lesort, "Least Squares Fitting of Circles," *J. Math. Imaging Vis.*, vol. 23, no. 3, pp. 239–252, 2005.
35. N. Chernov and C. Lesort, "Fitting ellipses, circles, and lines by least squares." 2008.
36. R. Siegwart and I. R. Nourbakhsh, *Introduction to Autonomous Mobile Robots*, 1st ed. A Bradford Book, 2004.
37. R. R. K. Meqdad Hamdan, "Method for Autonomous Picking of Paper Reels," Hamstad University, 2011.
38. K. I. Joy, "On-Line Geometric Modeling Notes,CUBIC UNIFORM B-SPLINE CURVE REFINEMENT," 2000.
39. wiki-Editors, Ed., "B-spline." 2011.
40. wiki-Editors, Ed., "Belt problem." 2011.

AUTHORS PROFILE

Meqdad Hamdan Hasan, Lecturer, Department of Building Engineering, Collage of Architecture and Planning, Imam Abdulrahman Bin Faisal University. Meqdad got his Bachelor's degree from Al-Balqa Applied University- College of Engineering Technology 2002. Then He got his master's degree from Halmstad University-Intelligent Systems Department 2011. He is a certified Professional Engineer and a member of the Jordanian Engineering Association since 2002.